

# The effectiveness of oyster filler on the physical and mechanical properties of novel dental restorative composite

Cite as: AIP Conference Proceedings **2290**, 050001 (2020); <https://doi.org/10.1063/5.0031467>  
 Published Online: 04 December 2020

Rafid M. AlBadr, Sadam A. Halfi, and Kareema M. Ziadan



View Online



Export Citation



**Your Qubits. Measured.**  
 Meet the next generation of quantum analyzers

- Readout for up to 64 qubits
- Operation at up to 8.5 GHz, mixer-calibration-free
- Signal optimization with minimal latency

[Find out more](#)





# The effectiveness of oyster filler on the physical and mechanical properties of novel dental restorative composite

Rafid M. AlBadr<sup>1,a)</sup>,Sadam A. Halfi<sup>2</sup> ,Kareema M. Ziadan<sup>2</sup>

<sup>1</sup>College of Dentistry, University of Basrah, Basrah, Iraq

<sup>2</sup>Department of Physics, College of Science, University of Basrah, Basrah, Iraq

a) Corresponding author: rafid.bader@uobasrah.edu.iq

**Abstract.** The objective of this paper was to investigate a blend of natural biomaterial such as oyster, which has wide availability, is low in cost, and is polymer-based, in order to obtain a dental composite with good physical and mechanical properties. Oyster shell was cleaned then crushed and milled ground by size less than 25 $\mu$ m. The average crystalline size of Oyster shell powder was examined using X-ray diffraction (XRD) showed peaks that were characteristic of calcium carbonate, morphology was examined using scanning electron microscopy also to know the composition of Oyster shell filler used EDX, also the specific surface area of the Oyster shell powder was analysed using BET analysis and FTIR was performed to identify the functional group. All test conducted has shown that oyster shells powder is mostly composed of calcium carbonate (CaCO<sub>3</sub>) with rare impurities and possibility to develop oyster powder as a filler. Physical and mechanical properties of the dental oyster composite were measured such as depth of cure and water absorption, and mechanical properties such as flexural strength, flexural modulus, and DTS, where observed. Experimental results confirmed that composites produced from a combination of the oyster powder indicated that the depth of cure behaviour of the composite decreased (2.36 $\pm$ 0.16 mm), while the water absorption properties of the composite increased 34.88 $\pm$ 2.75 and 4.29 $\pm$ 66  $\mu$ g/mm<sup>3</sup> for sorption and solubility respectively, increase in flexural strength (76.92 $\pm$ 5.42MPa), flexural modulus (14.571.31 GPa) occurred, as well as in DTS (46.40 $\pm$ 5.43MPa). Finally, all oyster composite values were ranged using the ISO 4904: 2008 requirement, as well as ANSI/ADA specification No. 27, for cure resins..

**Keywords:**Oyster, CaCO<sub>3</sub>, Dental Composites, SEM, FTIR, RDX, Physical properties, Mechanical properties.

## INTRODUCTION

One of the most important contributions of dentistry has been the resin compound technique, and how to improve its physical and mechanical properties. Several studies have been conducted to detect biomineralization processes, and these have also been greatly improved, alongside the production of a new generation of biomaterials. In the past decades, the use of natural biogenic structures and materials such as corals [1, 2], seashells [3], animal bones [4, 5], cuttlefish bone [6, 7], and bird eggshells and land snail shells [8] for medical purposes has been motivated by limitations in generating synthetic materials with the requisite structure and mechanical integrity. In terms of density, coral skeletons are a natural material that indicates the potential for the use in dental hard tissue restoration and augmentation. Nacre shells have also been studied for dentistry applications [9]. Coralline should be regarded as similar to alveolar sponge tissue and can be used for the regeneration of the jawbone, dentine, and periodontium [10]. Most dental composites are a blend of an acrylic monomer and particulate fillers that comprise silicate glasses (particle size of several microns), which are polymerized during application. Glassy fillers are not strong enough and exhibit cracks that either cut through glass fillers or propagate around filler particles [11]. To overcome this problem, many ideas have been suggested such as glass fibers, nanoporous fillers, branched fibers, and even using ceramic whiskers as filler [12]. The notion of utilizing porous fillers was first introduced by Bowen and Reed as a means for improving bonding between filler particles and the resin matrix [13,14]. Porous fillers used in this approach can be divided into

three categories: fillers with surface pores [11], fillers containing large and small particles sintered together [13], and fillers containing interconnected pores.

For the present study, we selected marine oyster shells, due to their wide availability and low cost, along with their biological-natural origin, which are highly attractive properties in the preparation of calcium phosphate powders for biomedical application. Additionally, oyster shell powder is used as a filler in various polymer materials for manufacturing composites such as polypropylene [14] and rubber composites [15]. Oyster shell is a biomaterial composed of 96%wt CaCO<sub>3</sub> and 4%wt other organic minerals in trace quantities, such as SiO<sub>2</sub>, Al<sub>2</sub>O<sub>3</sub>, Na<sub>2</sub>O, SrO, MgO, and SO<sub>3</sub> [16-18]. As such, the examination of oysters showed that attachment can be achieved with a chemically distinct, biomineralized material composed of predominantly inorganic (~86%) materials and significant levels of organic materials (~11%) [19]. Calcium carbonate is one of the most widely available biominerals. CaCO<sub>3</sub> is a shell candidate due to its relative ease of preparation, good environmental stability, and compatibility with other materials [20]; it also a type of light-colored mineral filler [21], and CaCO<sub>3</sub> partials comprise interconnected pores [22].

As manufacturers continue to search for a resin-based composite material with good physical properties and able to achieve teeth color, the introduction of new low cost and available materials has brought dentistry closer to achieving this goal. The purpose of this study was to use oyster shell which is characterized by easily prepared and good biocompatibility with an oral environment (Calcite and aragonite-based biomaterials). The oyster powder was examined by X-ray diffraction (XRD), scanning electron microscopy (SEM), Fourier Transform Infrared Spectroscopy (FTIR), BET and EDX. Then the experimental composite of oyster shell particles and Bis\_GMA(Bisphenol A-glycerolate dimethacrylate)/TEGDMA (TriethyleneGlycol Dimethacrylate) were prepared. The physical and mechanical properties of the dental composite, which contain oyster shell particles, were evaluated in this study

## EXPERIMENTAL

### Preparation and characterization of oyster powder

Twenty oysters from the north Arabian Gulf measuring 5cm to 8cm in length were thoroughly washed with water and impurities such as sand were removed. They were then dried and maintained for two weeks in the oven at 80°C to remove moisture. The external shell was filed by abrasion. The oysters were crushed below ~300µm using a mortar and pestle and were wet-milled in a planetary ball milling machine (RETSCH PM 100 Germany) for 2 hrs, then sieved using a 500-mesh sieve (openings < 25µm) to produce powder, as shown in Figure 1. This powder was determined for use as a filler in dental composite material.



**FIGURE. 1.** Image for the oysters: A: prior to scraping the shell; B: after scraping the shell; C: after milling (powder).

A scanning electron microscope (SEM) type VEGA TESCAN (Czech Republic) was used to characterize the morphology and size of the oyster powder. Additionally, an energy dispersive X-ray analyzer (EDX), linked to the SEM, was employed to semi-quantitatively investigate chemical compositions.

The specific surface area of oyster powder was computed by Brunauer-Emmett-Teller (BET) analysis. The BET method was used alongside a Chembet-3000 QUANTACHROME. The mean diameter (dBET) obtained by applying the BET method is represented as follows [23]:

$$d_{BET} = \frac{6}{A_s \rho} \quad (1)$$

Where  $A_s$  is the specific surface area (m<sup>2</sup>/g) and  $\rho$  is the theoretical density of the phase. Oyster powder density was measured using the pycnometric method, and was applied in ISO standard 1183-1:2004, and ASTM standard D854, with the uncertainty of  $\pm 0.02$  g/cm<sup>3</sup>.

X-ray diffraction (XRD) was performed using a Philips powder diffractometer with a copper (Cu K $\alpha$ ) X-ray source (Philips PW 1700 series diffractometer, Leiden, Netherlands). The oyster powder samples (< 25  $\mu$ m particle size) were scanned between  $2\theta$  (10° to 70°) with a step size of  $2\theta = 0.02^\circ$  in continuous mode and a count time of 0.35Sec per step. The crystallite size (D) of the glass samples was determined using the Scherrer equation [24]:

$$D = \frac{\beta \lambda}{W \cos \theta} \quad (2)$$

Where  $\lambda$  is the wavelength of the incident X-ray (0.154060 nm),  $\beta$  is Scherrer constant between 0.85 to 0.99, depending on the particle morphology ( $\beta = 0.89$  for spherical crystals with cubic symmetry),  $\theta$  is the diffraction angle, and  $W$  is the full width at half maximum (FWHM in radian).

Fourier-transform infrared analysis (FTIR; Nicolet Magna-IR 550 spectrometer, Madison, Wisconsin) was performed to identify the actual group of material and the chemical bonds between atoms.

## Preparation and characteristics of composites

The oyster powder particles' surface was pre-treated with silane-coupling 1.5wt% agent  $\gamma$ -methacryloxypropyltrimethoxy ( $\gamma$ MPS)), then blended with the matrix phase Bis\_GMA (2,2-Bis[4-2-hydroxy-3-methacryloxypropyl]phenyl]-propan)/TEGDMA(triethyleneglycol dimethacrylate). The weight ratio of filler was 76wt% (57% vol) of the resin. Camphorquinone (CQ) and dimethylaminoethylmethacrylate (DMAEMA) were added to the resin as catalysts to initiate and crosslink the composite.

Four specimens of the dental composite were prepared for the depth of cure measurements. The specimens were prepared in 4 mm diameter and 10 mm thicknesses, using a LED light unit source (Woodpecker, China, with an intensity of 600mW/cm<sup>2</sup>) for polymerization. The time for polymerization was 40 sec.

Sorption measurement specimens were prepared at 15 mm diameter and 1 mm thickness, using light-curing for both sides for 40 sec. They were then placed in a desiccator at 37°C and weighted after 24 hr. This cycle was repeated until a constant mass ( $m_0$ ) was obtained. Following on, the discs were immersed in distilled water at 37°C. The uptake of water was recorded until no further significant change in weight (equilibrium) was attained ( $m_1$ ). The measurements continued for roughly 90 days. The specimen discs were removed from the water and placed in a desiccator containing silica gel after one week and were weighed ( $m_2$ ). Sorption and solubility were calculated as follows [25]:

$$WA (\mu\text{g}/\text{mm}^3) = \frac{m_1 - m_2}{V} \quad (3)$$

$$WS (\mu\text{g}/\text{mm}^3) = \frac{m_0 - m_2}{V} \quad (4)$$

Flexural strength of the dental composites was conducted according to ISO 4049. The composite pastes were inserted into a specimen (2mm  $\times$  2mm  $\times$  25 mm) and were prepared in a mold using the light curing unit. An overlapping regime was applied to irradiate all the specimens on both sides; polymerization time was 40 sec. Specimens were stored in distilled water for 24 hr at 37°C; prior to testing, the three-point bending test was performed on the specimens, using a universal testing machine (Zwick/Roell BT1FR2.5TN, Germany) at a crosshead speed of 1 mm/min. The flexural strength (FS) in MPa was calculated as shown in the formula below [26]:

$$FS (MPa) = \frac{3FL}{2bd^2} \quad (5)$$

And

$$FM (GPa) = \frac{FL^3}{4bd^3p} \quad (6)$$

Where F is failure load (N), L is the distance between supports (20 mm), and b and d is width and thickness, respectively, of the specimens (mm). p is the deflexion corresponding to the load F (mm).

Diametral tensile strength test was measured for four specimens with a 6mm diameter and 4mm height, using light-curing for 40 sec on both sides. The curing specimens were stored in distilled water for 24 hr at 37°C, prior to testing. A universal testing machine (Zwick/Roell BT1FR2.5TN, Germany) was used for the test, at a crosshead speed of 1cm/min. The DTS (MPa) was computed as the formula below:

$$DTS (MPa) = \frac{2F}{\pi DL} \quad (7)$$

Where F is the load at fracture (N), and D and L are the diameter and height of specimens (mm), respectively.

## RESULTS AND DISSCASION

### Characterization of oyster powder

Figure 2 provides SEM images of the oyster specimens. The images show some particles in the shape of parallel rectangles; in addition, some particles had an irregular shape, with sharp edges. The particle size analysis using the NIH image program [27, 28], found the mean of particle distribution for the oyster powder to be 215.57±92.2nm (from approximately 200 particles). Figure 3 shows particles size distribution; only one peak centered at a range of 200 nm to 250 nm was observed, suggesting good distribution. The result for small particles indicated a large surface area with which to interact with coupling agent silane and can be homogeneously dispersed in the resin.

The particle size of the oyster powder was also estimated for the BET surface area by calculating an equivalent spherical diameter; the density of oyster powder was calculated as being 2.57± 0.28g/cm<sup>3</sup>. BET measurements of oyster powder yielded a specific surface area of 8.659 m<sup>2</sup>/g. Using equation 1, a particle size of ~269 nm was detected. From the BET analysis, it can be inferred that oyster powder is porous and as such, the surface area will be slightly elevated.

Figure 4 shows the XRD patterns for oyster powder and Hume peaks between 20° and 50° in the basal line. The identified XRD patterns of oyster powder corresponded to JCPDS files NO. 24 to 0027 for calcite, and 41 to 1475 and 5 to 453 for aragonite. Most peaks for the XRD patterns can, therefore, be assigned to aragonite crystals. Indeed, XRD analyses confirmed that the cellular basis of oyster formation that the polymorphs (calcite, vaterite, and aragonite) of calcium carbonate, and more formation of aragonite. Since the powder of CaCO<sub>3</sub> is maintained for two weeks in the oven at 80°C during preparation, the formation of crystalline CaCO<sub>3</sub> polymorphs and It will transform to calcite via vaterite moderate at low temperatures (≤30°C), and to aragonite via vaterite at higher temperatures (≥40°C) [29, 30].

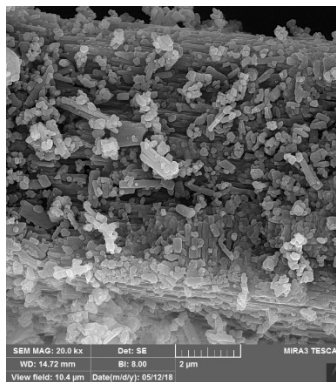


**FIGURE 2.** Scanning electron microscopy (SEM) images of the oyster sample.

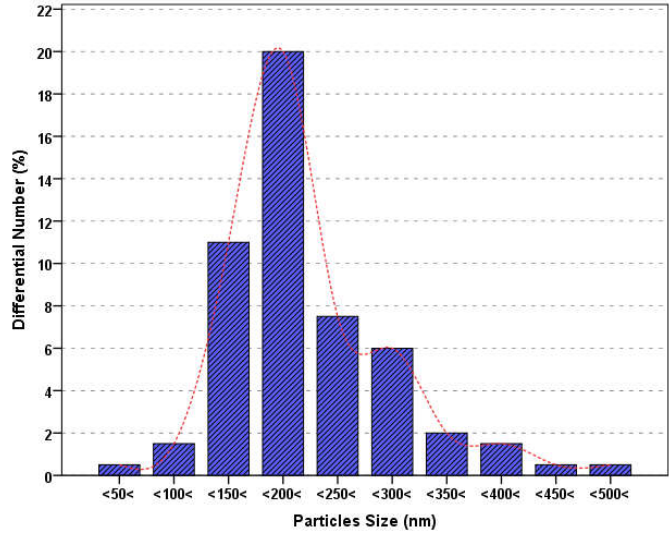


FIGURE 3. The particle size distribution of oyster shell powder.

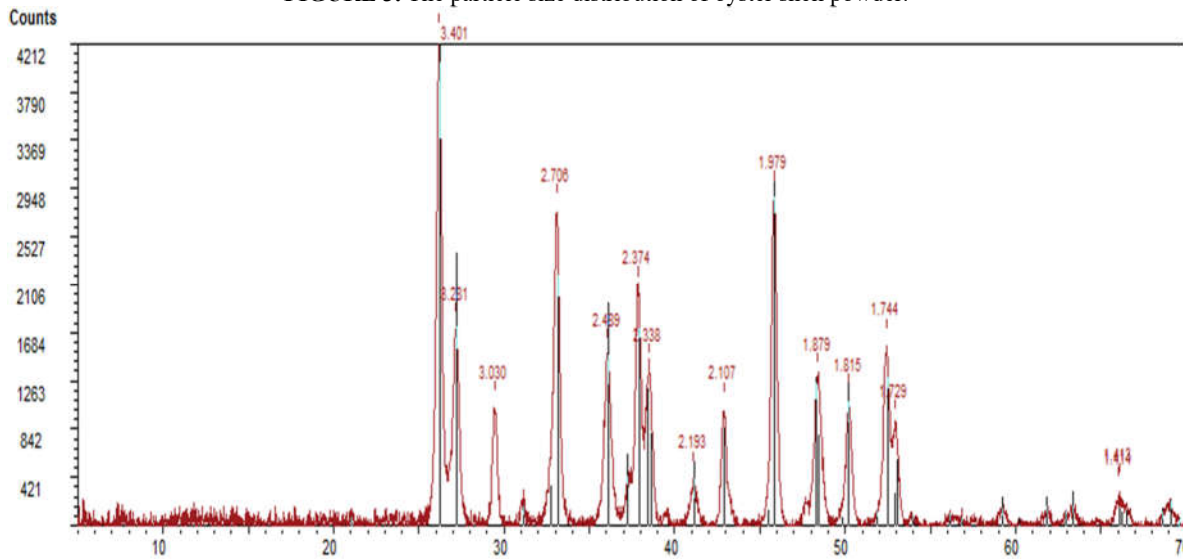


FIGURE 4. XRD patterns of oyster powder.

Figure 5 shows the EDX analyses for oyster powder. The overt presence of Ca, C, and O are indicated, which highlights the phenomenal dominance of aragonite and calcite in the oyster powder. This result confirms what was indicated in the XRD spectra. In addition, EDX analyses observed the presence of limited quantities of elements such as Na, Al, and Si. These results are shown in Table 1

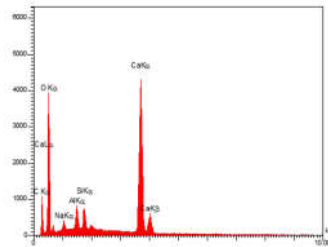
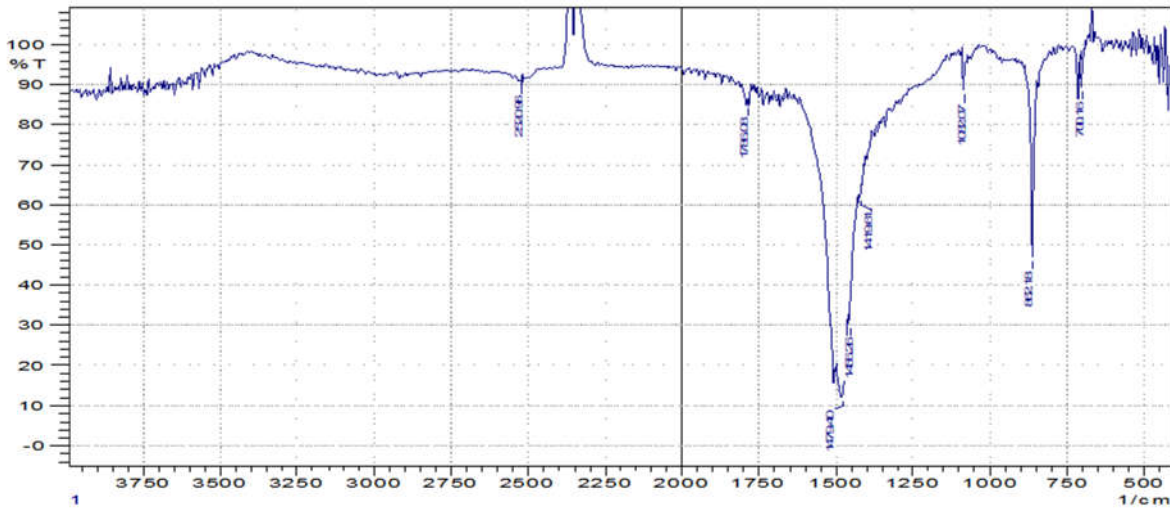


FIGURE 5. EDX spectral analyses of oyster powder.

**Table 1.** Elemental composition of the oyster powder.

Elements	W%	A%	Pk/Bg
C	6.94	11.73	225.69
O	49.38	62.64	1314.58
Na	3.08	2.72	53.19
Al	5.43	4.09	55.63
Si	4.73	3.41	45.31
Ca	30.44	15.41	174.36

Figure 6 shows that FTIR spectra exhibited infrared bands related to oyster phase, located at 700, 862, 1082, 1420, 1456, 1478, 1786, and 2520 cm<sup>-1</sup>. These observed peaks are noted in Table 1. From the ratios of peak intensities, the CaCO<sub>3</sub> of oyster powder appears to be ~2/3 aragonite and ~1/3 calcite.



**Figure 6.** The FTIR spectra of the oyster powder sample.

**Table 2.** FTIR spectral absorption of oyster powder.

Wave number [cm <sup>-1</sup> ]	Functional group
700	Aragonite (v4)
862	Carbonate out-of-plane bending vibration (v2) (aragonite)
1082	Amorphous calcium carbonate (aragonite) and v1 symmetric stretching vibration [31]
1419-1478	Asymmetric stretch of the carbonate ion (v3)[32]) (aragonite) (calcite)
1766	The asymmetric stretch of the carbonate ion (v1 +v4) (calcite) [33]
2700-3600	(O-H stretching)

The characterization of oyster powder is shown in Table 3. The result indicates that the oyster powder can serve as a good filler in dental composites.

Surface treatment with the silane coupling agent for oyster powder is essential to improve the consistency between oyster powder filler and resin. Oyster powder's primary component was shown to be CaCO<sub>3</sub>, which had poor interaction with the acrylic monomer. Interestingly, the mechanical properties of composite failed or decreased when the silane coupling agent was not properly modified for the entire oyster powder surface.

**Table 3.** Properties of oyster fillers.

	Density [g/Cm <sup>3</sup> ]	$d_{XRD}$ [nm]	BET [m <sup>2</sup> /g]	$d_{BET}$ [nm]	$d_{SEM}$ [nm]
Oyster powder	2.57 ± 0.28	32.583	8.659	269	215.57 ± 92.2

## Properties of dental composites

Oyster (CaCO<sub>3</sub> particles) filler, like most inorganic materials, have a polar, hydrophilic, and high-energy surface that tends to conglomerate, causing inherent structural defects in composites [34, 35].

The depth of cure for the oyster composite according to ISO 4049:2000, the deeper denoted  $2.3567 \pm 0.166$  mm. The result of low in depth cure; this was due to minor non-symmetrical (LED\_curing lamp) light distribution from the centre of the sample. Additionally, the oyster powder filler was a turbid powder, giving rise to a non-bright white composite when polymerization scattered the light, causing it to not penetrate deeply into the filling.

Water sorption and solubility behaviour are very important properties that must be considered for selecting dental composites. These characteristics provide clear information on the kinetic nature of water on composites in an oral environment. The results for water sorption and solubility were  $34.884 \pm 2.756$  and  $4.2207 \pm 0.664$   $\mu\text{g}/\text{mm}^3$ , respectively. For sorption rate, a slightly higher value was observed, this resulting, corresponding to the micro particles retain ,high sorption ability with respect to water, as well as because of diffusion of ionic salts within the matrix which form CaCO<sub>3</sub> crystal structure within the matrix, also ,a proper distribution of filler in matrix of composite contributes directly to the decrease water sorption which attributed accumulation of oyster powder filler in place and penetrating the water molecules inside it. Furthermore, these values were lower than the maximum value required by the ISO 4049 standard, i.e.  $< 40$   $\mu\text{g}/\text{mm}^3$  for sorption and  $< 7.5$   $\mu\text{g}/\text{mm}^3$  for solubility [36].

The flexural strength of oyster powder filler-based composites was evaluated, and the results were  $76.9215 \pm 5.424$  MPa for flexural strength. The increase in flexural strength, with a corresponding increase in filler content, may relate to the fact that when oyster shell powder filler was added to the polymer system, it acted as a binder, which lowered the elasticity of the polymer matrix and increased the absorption ability of the composite. in this study, oyster shell composite investigated showed flexural strength values passed the requirements of ISO 4049 for polymer-based restoratives classifies dental polymer-based restorative materials which requested a record of flexural strength is more than 50MPa. However, the flexural modulus was denoted  $14.575 \pm 1.311$  GPa. It is clear that the oyster powder filler loading improves the mechanical properties of the composite.

Diametral tensile strength (DTS) was measured as  $46.4038 \pm 5.435$  MPa. DTS is used to better understand the behaviour of brittle materials. The result of DTS was acceptable for dental composites limited to 30 to 55 MPa [37].

The oyster powder filler was porous (base CaCO<sub>3</sub>), which slightly increased mechanical properties such as flexural strength; this can be explained as the result of incomplete penetration of resins into the filler pores. Furthermore, the empty pores acted as voids in the system, causing weak points in the composite structure. The bond between fillers and resins in dental composites is very important. Using porous fillers, with good penetration of resin into fillers, a reliable and strong bond can be created between two components [11]. The results also showed that the porosity of the oyster filler did not significantly affect the DTS.

## CONCLUSION

The results of this study indicate that oyster powder can potentially be a good filler in the preparation of dental composites. It can potentially enhance flexural strength and flexural modulus; however, these aspects may decrease along with the depth of cure. The sorption of water in composites was increased with the addition of oyster powder. However, water sorption level in composites within specification IOS4049 for resin. Finally, the composites with oyster filler were overall effective, and may, therefore, be a promising material for restorative dental materials, due to its low cost and good physical and mechanical properties in the range of ISO4049. Further research is needed to review the use of natural biogenic structures in dentistry, and to investigate the nature of its composition and its dental properties.



## REFERENCES

1. Hu, J., J. Russell, B. Ben-Nissan, and R. Vago, *J Mater Sci Lett*, 20, 1 (2001).
2. Xu, Y., D. Wang, L. Yang, and H. Tang, *Mater Charact*, 47, 2 (2001).
3. Vecchio, K.S., X. Zhang, J.B. Massie, M. Wang, and C.W. Kim, *Acta Biomater*, 3, 6 (2007).
4. Murugan, R., S. Ramakrishna, and K.P. Rao, *Mater Lett*, 60, 23 (2006).
5. Göller, G., F.N. Oktar, S. Agathopoulos, D. Tulyaganov, J.M.F. Ferreira, E. Kayali, and I. Peker. *The influence of sintering temperature on mechanical and microstructural properties of bovine hydroxyapatite*. in *Key Eng Mater*. 2005: Trans Tech Publ.
6. Rocha, J., A. Lemos, S. Agathopoulos, P. Valério, S. Kannan, F. Oktar, and J. Ferreira, *Bone*, 37, 6 (2005).
7. Zhang, X. and K.S. Vecchio, *J Cryst Growth*, 308, 1 (2007).
8. Salma-Ancane, K., L. Stipnice, and Z. Irbe, *Ceram Int*, 42, 8 (2016).
9. Langer, R., *Adv Mater*, 21, 32-33 (2009).
10. Green, D.W., W.-F. Lai, and H.-S. Jung, *Mar Drugs*, 12, 5 (2014).
11. Zandinejad, A., M. Atai, and A. Pahlevan, *Dent Mater*, 22, 4 (2006).
12. Roberson, T., H. Heymann, and E. Swift, Louis: Mosby, (2000).
13. Hengchang, X. and J. Nagel, Editor^Editors. 1998, Google Patents.
14. Prabhakar, M., D.-W. Lee, B.-S. Kim, and J.I. Song, *Composites Research*, 27, 5 (2014).
15. Li, L., Z. Zeng, Z. Wang, Z. Peng, X. She, S. Li, and J. Zhong, *Polymers & Polymer Composites*, 25, 1 (2017).
16. Wu, S.-C., H.-C. Hsu, Y.-N. Wu, and W.-F. Ho, *Mater Charact*, 62, 12 (2011).
17. Al-Sayed, H.A., A.M. Mahasneh, and J. Al-Saad, *Mar Pollut Bull*, 28, 6 (1994).
18. Nwanonenyi, S., M. Obidiegwu, T. Onuchukwu, and I. Egbuna, *The International Journal Of Engineering And Science*, 2, 7 (2013).
19. Burkett, J.R., L.M. Hight, P. Kenny, and J.J. Wilker, *J Am Chem Soc*, 132, 36 (2010).
20. Zhao, W., H. Yang, and C. Huo, *Colloids Surf Physicochem Eng Aspects*, 393, (2012).
21. Petrack, J., M. Vucak, C. Nover, and M. Epple, *J Appl Polym Sci*, 132, 1 (2015).
22. Gong, J., T. Liu, D. Song, X. Zhang, and L. Zhang, *Electrochem Commun*, 11, 10 (2009).
23. Rouquerol, J., F. Rouquerol, P. Llewellyn, G. Maurin, and K.S. Sing. 2013: Academic press.
24. D.CULLITY, B. 1956: ADDISON-WESLEY PUBLISHING COMPANY.
25. Al-Bader, R.M., K.M. Ziadan, and M. Al-Ajely, *International Journal of Medical Research and Health Sciences*, 4, 2 (2015).
26. Atai, M., A. Pahlavan, and N. Moin, *Dent Mater*, 28, 2 (2012).
27. Abrâmofoff, M.D., P.J. Magalhães, and S.J. Ram, *Biophotonics international*, 11, 7 (2004).
28. Rasband, W., There is no corresponding record for this reference, (2011).
29. Ogino, T., T. Suzuki, and K. Sawada, *Geochim Cosmochim Acta*, 51, 10 (1987).
30. Rodriguez-Blanco, J.D., S. Shaw, and L.G. Benning, *Nanoscale*, 3, 1 (2011).
31. Su, J., F. Zhu, G. Zhang, H. Wang, L. Xie, and R. Zhang, *CrystEngComm*, 18, 12 (2016).
32. Addadi, L., S. Raz, and S. Weiner, *Adv Mater*, 15, 12 (2003).
33. White, W. and V. Farmer, *Mineralogical Society Monograph*, 4, (1974).
34. Maiti, S. and P. Mahapatro, *J Appl Polym Sci*, 42, 12 (1991).
35. Feng, J., M. Chen, and Z. Huang, *J Appl Polym Sci*, 82, 6 (2001).
36. ISO4049., Editor^Editors. 2000.
37. Powers, J.M. and R.L. Sakaguchi, 13 ed. 2012: Elsevier India.